Modeling the microstructure and elastic properties of complex materials

by

A. P. Roberts
Centre for Microscopy and Microanalysis
University of Queensland
St. Lucia, Queensland 4072, Australia

and

E. J. Garboczi
Building and Fire Research Laboratory
National Institute of Standards and Technology
Gaithersburg, MD 20899 USA

Reprinted from MSM 2000 International Conference on Modeling and Simulation of Microsystems. Proceedings. Applied Computational Research Society. March 27-29, 2000, San Diego, CA, 2000.

NIST
National Institute of Standards and Technology
Technology Administration, U.S. Department of Commerce

Modeling the microstructure and elastic properties of complex materials

A. P. Roberts*,† and E. J. Garboczi*

*Building Materials Division, National Institute of Standards and Technology, Gaithersburg, MD 20899, USA, Edward.Garboczi@nist.gov
†Centre for Microscopy and Microanalysis, University of Queensland, St. Lucia, Queensland 4072, Australia, anthony.roberts@mailbox.uq.edu.au

ABSTRACT

The finite element method is used to study the influence of porosity and pore shape on the elastic properties of model porous media. The Young's modulus of each model was found to be practically independent of the solid Poisson's ratio. The results are in good agreement with experimental data. We provide simple formulae that can be used to predict the elastic properties of porous media, and allow the accurate interpretation of empirical data in terms of pore shape and structure.

Keywords: elastic moduli, finite-element method, porous media, ceramics, foams, random materials.

1 Introduction

Materials with complex microstructure arise in a wide range of applications. Materials include ceramics, foamed solids, aerogels, polymer blends, and artificial bone [1]–[3] If a material is to be synthesized for a particular purpose, it is important to understand the relationship between microstructure and the target property. Generally, theoretical relationships only account for porosity, although the shape and nature (e.g. connectivity) of the the porosity and solid phase are known to be critical. In this study, we use the finite element method to study the relationship between microstructure and the bulk elastic properties of a wide range of realistic porous models.

There have been several different approaches to deriving property-porosity relations for random porous materials. Formulae derived using the *micro-mechanics* method [4] are essentially various methods of approximately extending exact results for small fractions of spherical pores to higher porosities. A drawback of this approach is that the microstructure corresponding to a particular formula is not precisely known; hence agreement or disagreement with data can neither confirm nor reject a particular model. A second class of models, based on periodic microstructures (for example arrays of spheres or repeated cell-units), are often too simple to mimic the complex microstructures found in real materials. Finally, there do exist rigorous theories based on microstructural inputs [3], but the information required to evaluate the results is generally difficult to obtain. The most promising results in this class are variational bounds [1], [3].

Another approach is to computationally solve the equations of elasticity for digital models of microstructure [5]. In principle this can be done exactly. However, large statistical variations and insufficient resolution have limited the accuracy of results obtained to date. Only recently have computers been able to handle the large 3-D models and number of computations needed to obtain reasonable results. As input to the method, we employ nine different microstructural models that broadly cover the types of morphology observed in porous materials. The results, which can be expressed simply by two parameter relations, correspond to a particular microstructure and explicitly show how the properties depend on the nature of the porosity. Therefore, the results can be used as a predictive tool for cases where the microstructure of the material is similar to one of the models, and as an interpretive tool if the microstructure is unknown.

2 Results and discussion

The models we consider are depicted in Fig. 1. The models are digitized on grids of a sufficiently high resolution to capture the important details of the model. This study is limited to grids of linear dimension $M \leq 128$ (ie. $M^3 \approx 2 \times 10^6$ pixels). The finite element method (FEM) uses a variational formulation of the linear elastic equations, and finds the solution by minimizing the elastic energy via a fast conjugate gradient method. A strain is applied, with the average stress or the average elastic energy giving the effective elastic moduli [1], [3]. Details of the theory and programs used are reported in Ref. [5]. The actual programs are available at *http://ciks.cbt.nist.gov/garboczi/*, Part II Chapter 2.

Results for the "Boolean" models (overlapping solid sphere, spherical pores and ellipsoidal pores) are shown in Fig. 2. Each symbol represents the average over five different samples to reduce statistical errors in the results. We study the models for reduced densities $p = \rho/\rho_s > 0.5$, where ρ and ρ_s are the density of the porous media and solid matrix respectively. It becomes increasingly difficult to make accurate measurements at low densities as the properties depend more and more on thin connections which are difficult to accurately resolve. The density range we study encompasses most

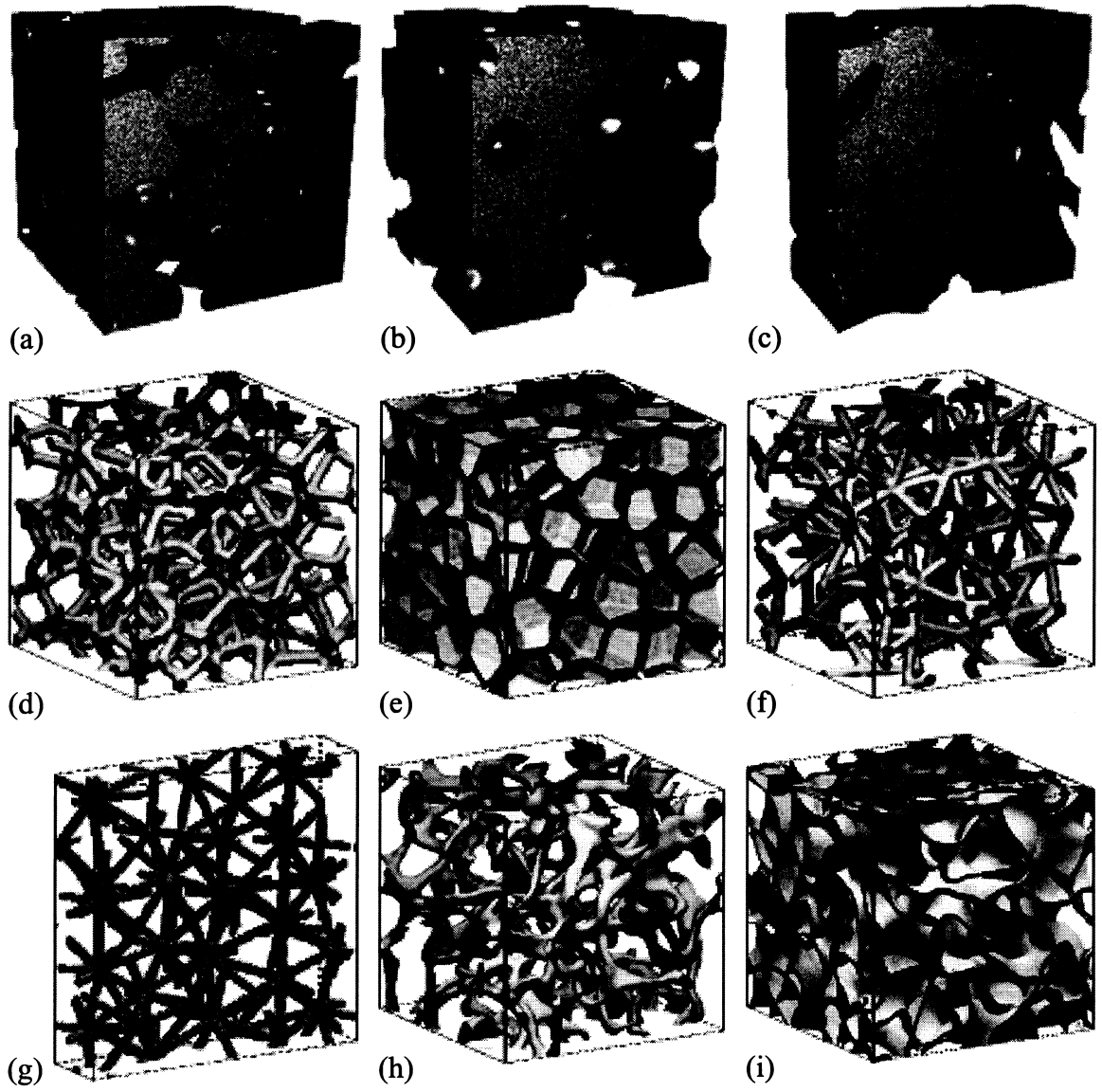

Figure 1: The model microstructures. (a) overlapping solid spheres, (b) overlapping spherical pores, (c) overlapping ellipsoidal pores, (d) open-cell Voronoi tessellation, (e) closed-cell Voronoi tessellation, (f) open-cell node-bond model, (g) open-cell node-bond model, (h) open-cell level-cut Gaussian random field, and (i) closed-cell level-cut Gaussian random field. The Boolean models (a–c) are discussed in Refs. [3], [6] and the Voronoi tessellation (d–e) is reviewed by Stoyan *et al* [6]. The node-bond models (f–g) will be described in a forthcoming paper [7] and the details of the level-cut Gaussian random field scheme we use is reported in Ref. [8]

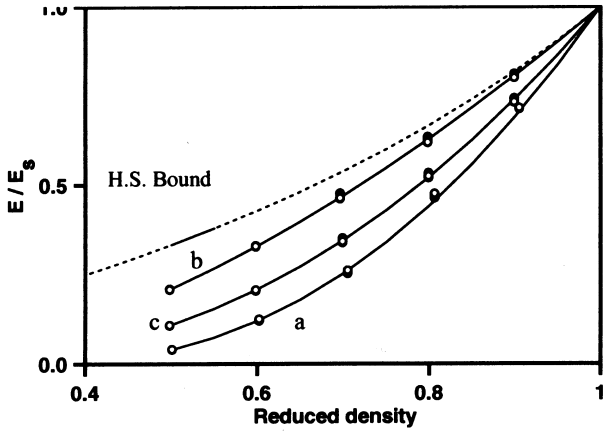

Figure 2: The Young's modulus of the Boolean models shown in Fig. 1. The almost overlapping symbols at each point correspond to different solid Poisson's ratios. The dotted line is the Hashin-Shtrikman upper-bound [1] for isotropic media.

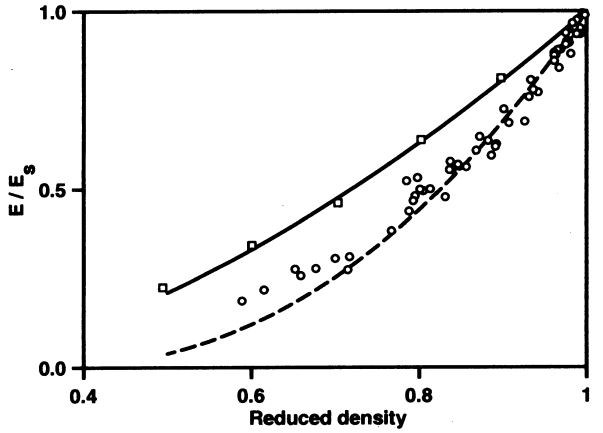

Figure 3: Experimental data for porous alumina compared with the overlapping spherical pore (——, Fig. 1b) and solid sphere models (– – –, Fig. 1a).

sintered ceramics, with which we compare our results below. The density dependence of the Young's modulus can be fitted with the equation

$$E/E_s = ((p - p_0)/(1 - p_0))^m \qquad (1)$$

where p_0 and m are reported in Table 1. Here E (E_s) is the Young's modulus of the porous medium (solid matrix). Note that m and p_0 are empirical correlation parameters and should not be interpreted as the percolation exponent and threshold, respectively. The FEM results shown in the figure took approximately four thousand hours to compute on current high-end workstations.

In Figure 3 we compare the results to experimental data for porous alumina [9], [10]. Most of the data falls

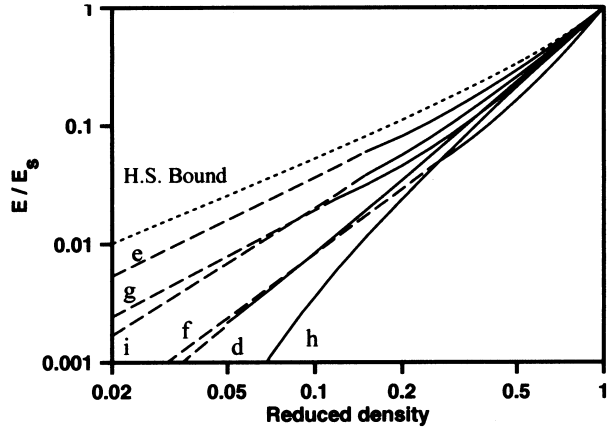

Figure 4: The Young's modulus of the cellular models shown in Figs. 1(d–i). The solid and dashed lines correspond to the empirical fits given in Table 1.

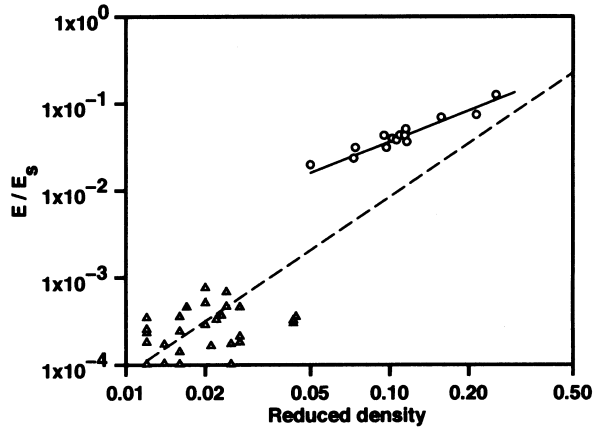

Figure 5: Experimental data for open- (○) and closed-cell (△) cellular solids compared with the FEM results for open- (– – –, Fig. 1d) and closed-cell (——, Fig. 1e) Voronoi tessellations.

close to the line for overlapping solid spheres (Fig. 1a). Many of these ceramics are synthesized by sintering a ceramic powder, consistent with the model microstructure. The additional data [9] are for a material made with a particulate filler, which should give a microstructure similar to that observed in the overlapping spherical pore model (Fig. 1b). The FEM result for this model is seen to agree well with the data.

We have also studied the properties of six different models of cellular solids [2]. At high densities the data can be described by Eq. (1) with the parameters reported in Table 1. The density range where Eq. (1) remains accurate is also given. Since cellular solids can have extremely low densities (e.g. $p \approx 0.01$ for open-cell materials), it is necessary to obtain results at lower densities. For each of the models the FEM results appear to adopt a linear behaviour on a log-log graph as

$p \to 0$, indicating a conventional scaling fit of the form [2] $E/E_s = Cp^n$. The parameters C and n, and the applicable density range, are given for each of the cellular models in Table 1.

In Fig. 5 we compare selected FEM results for the cellular models with experimental data. The Young's modulus of closed-cell foamed glass [11] agrees well with results for the closed-cell Voronoi tesselation (Fig. 1e). Moreover, micrographs of the glass [11] show a structure similar to that of the model. Data for open-cell materials [2] show considerable scatter, but appear to be reasonably well modelled by the open-cell Voronoi tessellation (Fig. 1d).

We have also studied the influence of solid Poisson's ratio ν_s on the Young's modulus. The Young's modulus at $\nu_s = [-0.1, 0.0, \ldots, 0.4]$ is plotted in Fig. 2. At a given density the results are practically indistinguishable, indicating that E is nearly independent of ν_s. Therefore, the empirical formulae given in Table 1 can be applied to solids with arbitrary Poisson's ratios. Exact calculations for the modulus of a matrix containing dilute spherical pores [1] actually show a small dependence on ν_s, indicating that the result is only approximately true.

The models we have considered above are qualitatively similar to the microstructures observed in real composites. However, it is also important to establish a quantitative link with experimental characterization data. This may be done by tuning the parameters of a 3-D model so that its statistical microstructure properties match those of a 2-D micrograph. As an example, we show a porous tungsten matrix and its 3-D statistical reconstruction in Fig. 6 (the details are given in Ref. [8]). The finite-element code is then used to measure the Young's modulus of the model giving E/E_s=0.57 (where we have used a solid Poisson's ratio of $\nu = 0.28$). This compares well with the experimental value of E/E_s=0.59. The process of measuring the statistical properties of a given material, generating a corresponding model, and measuring its properties is time intensive. It is expected that future research will make the method more efficient.

We have derived emprical finite-element theories that explicity show the connection between density, microstructure, and the Young's modulus of complex porous materials. The results may be used to predict the properties of porous materials, or accurately interpret experimental measurements. The results will be described in greater detail in a forthcoming publication [7].

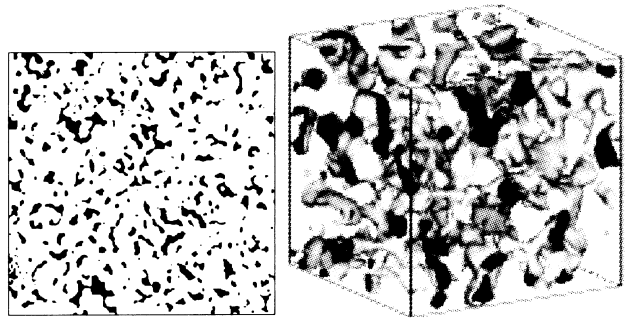

Figure 6: A two dimensional image (left) of a tungsten matrix [12] (the black regions represent pores). A 3-D model which shares statistical properties with the experimental image [8].

Table 1: For low densities ($p < p_{\max}$) the finite-element data can be described by $E/E_s = Cp^n$. At high densities ($p > p_{\max}$) the relation $E/E_s = [(p-p_0)/(1-p_0)]^m$ is used. The parameters correspond to the models listed in the first column.

	$p < p_{\max}$			$p > p_{\min}$		
Fig.	n	C	$p_{\max}$	m	p_0	$p_{\min}$
1(a)				2.23	0.652	0.50
1(b)				1.65	0.818	0.50
1(c)				2.35	0.798	0.50
1(d)	2.0	0.93	0.50	2.12	-0.0056	0.04
1(e)	1.2	0.56	0.30	1.19	-0.196	0.15
1(f)	1.8	0.54	0.35	4.27	-0.445	0.25
1(g)	1.3	0.38	0.25	2.80	-0.198	0.10
1(h)	3.2	4.2	0.20	2.15	0.029	0.05
1(i)	1.5	0.69	0.20	1.54	-0.121	0.15

REFERENCES

[1] Z. Hashin, J. Appl. Mech. **50**, 481 (1983).

[2] L. J. Gibson and M. F. Ashby, *Cellular solids: Structure and properties* (Pergamon Press, Oxford, 1988).

[3] S. Torquato, Appl. Mech. Rev. **44**, 37 (1991).

[4] R. M. Christensen, *Mechanics of composite materials* (Wiley, New York, 1979).

[5] E. J. Garboczi and A. R. Day, J. Mech. Phys. Solids **43**, 1349 (1995).

[6] D. Stoyan, W. S. Kendall, and J. Mecke, *Stochastic geometry and its applications*, 2nd ed. (Wiley, Chichester, 1995).

[7] A. P. Roberts and E. J. Garboczi (unpublished).

[8] A. P. Roberts and E. J. Garboczi, J. Mech. Phys. Solids **47**, 2029 (1999).

[9] R. L. Coble and W. D. Kingery, J. Am. Ceram. Soc. **39**, 377 (1956).

[10] F. P. Knudsen, J. Am. Ceram. Soc. **45**, 94 (1962).

[11] J. G. Zwissler and M. A. Adams, in *Fracture Mechanics of Ceramics*, edited by R. C. Bradt, A. G. Evans, D. P. H. Hasselman, and F. F. Lange (Plenum Press, New York, 1983), Vol. 6, pp. 211–241.

[12] S. Umekawa, R. Kotfila, and O. D. Sherby, J. Mech. Phys. Solids **13**, 229 (1965).